Prospects of Phase Resolved Optical Emission Spectroscopy as a Powerful Diagnostic Tool for RF-Discharges

T. Gans*, V. Schulz-von der Gathen, H.F. Döbele

Institut für Laser- und Plasmaphysik, Universität Essen, Germany

Phase resolved optical emission spectroscopy (PROES) bears considerable potential for diagnostics of RF discharges that give detailed insight of spatial and temporal variations of excitation processes. Based on phase and space resolved measurements of the population dynamics of excited states several diagnostic techniques have been developed. Results for a hydrogen capacitively coupled RF (CCRF) discharge are discussed as an example. The gas temperature, the degree of dissociation and the temporally and spatially resolved electron energy distribution function (EEDF) of energetic electrons (>12eV) are measured. Furthermore, the pulsed electron impact excitation during the field reversal phase, typical for hydrogen CCRF discharges, is exploited for measurements of atomic and molecular data like lifetimes of excited states, coefficients for radiationless collisional de-excitation (quenching coefficients), and cascading processes from higher electronic states.

1 Introduction

RF discharges bear a considerable application potential [1]. Investigations by optical emission spectroscopy (OES) can be fairly complicated due to pronounced spatial and temporal variations of various excitation processes over the RF cycle. Temporal variations are not considered in the standard corona model commonly used for OES of low-density plasmas, since it is based on balance equations only. Phase resolved OES (PROES) requires a time dependent model based on rate equations.

2 Model for PROES

An analytical model for the population dynamics during the RF cycle has been developed. The model takes into account: electron impact excitation, heavy particle collisional excitation, radiationless collisional de-excitation (quenching), radiation trapping and cascading processes from higher electronic states. Electron impact $(E^e(t))$ and heavy particle collisional excitation $\left(E^H(t)\right)$ out of the ground state are described by the excitation function $E(t) = E^e(t) + E^H(t)$. Excitation out of metastable or resonant states can be included in gerneral. However, these processes are negligible in molecular discharges at elevated pressure - as the investigated hydrogen CCRF discharge - because of low population densities of these states due to effective quenching processes by molecules [2].

For an excited state i not populated by cascade processes the excitation function $E_i(t)$ can be determined directly from the measured number of photons per unit volume and time $\dot{n}_{Ph,i}(t)$:

$$E_i(t) = \frac{1}{n_0 A_{ik}} \left(\frac{d\dot{n}_{Ph,i}(t)}{dt} + A_i \dot{n}_{Ph,i}(t) \right) \quad . \tag{1}$$

Here, $\dot{n}_{Ph,i}(t) = A_{ik} n_i(t)$ is given by the transition probability A_{ik} of the observed emission and the population of the investigated state $n_i(t)$; n_0 is the ground state density. The effective decay rate $A_i = \sum_k A_{ik} g_{ik} + \sum_q k_q n_q$

* permanent address: Institut für Plasma- und Atomphysik, Ruhr-Universität Bochum, Germany; e-mail address: timo.gans@web.de

takes into account spontaneous emission, radiation trapping and quenching. g_{ik} is the so-called escape factor and k_q the quenching coefficient with species q of the density n_q.

For quantitative investigations of the population dynamics cascade processes can be substantial [3, 4, 5, 6, 7]. The population density $n_i(t)$ of the investigated state i can be described by the following rate equation including cascades from state c:

$$\frac{dn_i(t)}{dt} = n_0 E_i(t) - A_i n_i(t) + A_{ci} n_c(t) \qquad . \tag{2}$$

The population density $n_c(t)$ obeys a rate equation analogous to eq. 2, without cascade processes. The coupled differential equations for the investigated state i and the cascade state c can be solved in a general manner for the periodic boundary conditions of an RF discharge ($n_{i,c}(t) = n_{i,c}(t+T)$):

$$\begin{aligned} n_i(t) &= n_0 \left(\frac{\widetilde{E_i}(T, A_i) e^{-A_i T}}{1 - e^{-A_i T}} + \widetilde{E_i}(t, A_i) \right) e^{-A_i t} \\ &+ \frac{n_0 A_{ci}}{A_i - A_c} \left[\left(\frac{\widetilde{E_c}(T, A_c) e^{-A_c T}}{1 - e^{-A_c T}} + \widetilde{E_c}(t, A_c) \right) e^{-A_c t} \right. \\ &\left. - \left(\frac{\widetilde{E_c}(T, A_i) e^{-A_i T}}{1 - e^{-A_i T}} + \widetilde{E_c}(t, A_i) \right) e^{-A_i t} \right] . \end{aligned} \tag{3}$$

Here, the abbreviation $\widetilde{E_x}(t, A_y) = \int_0^t E_x(t') e^{A_y t'} dt'$ has been used. Together with analytical approximations for time dependencies of excitation processes, eq. 3 allows us to determine amplitudes of excitation processes even for states fed by cascade processes. Additionally, this access to excitation functions is less sensitive to noise in measurements than the direct one (eq. 1), because derivatives of measured data are avoided.

3 Experiment

PROES measurements are performed in a CCRF discharge excited at 13.56 MHz in hydrogen with small admixtures of rare gases. The setup is described in detail elsewhere [11]. The flat, cooled stainless steel electrodes are 25 mm apart and 100 mm in diameter. The discharge is excited asymmetrically with one electrode grounded. The discharge axis is imaged onto the entrance slit of a 2m-spectrograph. A fast gateable ICCD-camera (LaVision Picostar, gate: 3 ns, repetition rate: 13.56 MHz) samples spectral intervals of about 4.5 nm with a spectral resolution of 0.03 nm and a spatial resolution of about 0.5 mm. The entire optical system is calibrated with a tungsten ribbon lamp.

4 Results

Fig. 1 displays the phase resolved emission of the n=3 level of atomic hydrogen along the discharge axis, at 141 Pa and 100 W. The abscissa comprises two RF periods (74ns each). Structures I and II are caused by electron impact excitation during the field reversal phase, typical for hydrogen CCRF discharges, and the sheath expansion phase, respectively [8]. Structure III results from fast secondary electrons created by ion impact at the powered electrode and ionisation in the sheath region [9]. Structure IV is related to heavy particle collisional excitation of energetic (>100eV) hydrogen atoms created at the electrode surface by impact of hydrogen ions [10].

The strong pulsed electron impact excitation in front of the powered electrode during the field reversal phase (structure I) induces a high population of excited states. De-excitation processes of these states and population by cascading processes can be investigated quantitatively in an interval practically free of electron impact excitation after the pushing out of electrons during the sheath expansion phase.

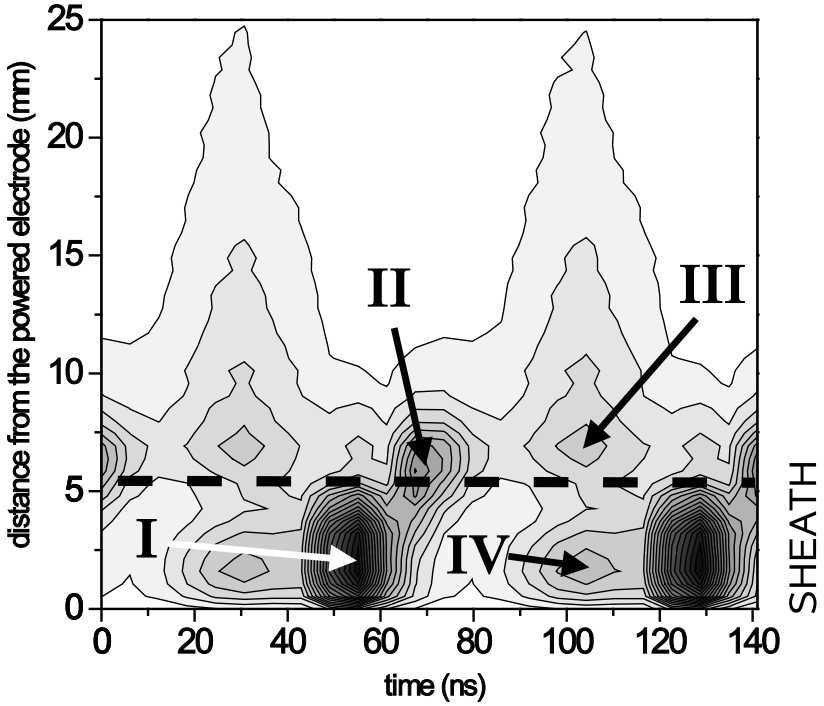

Fig. 1 Space and time resolved emission of Balmer-α from a CCRF hydrogen discharge operating at 141 Pa and 100 W.

4.1 Lifetimes and quenching coefficients

The population dynamics of excited states in the electron free interval after the sheath expansion phase is mainly determined by the effective decay rate A_i. Detailed consideration of population processes by cascades and heavy particle collisions with eq. 3 is described elsewhere [7]. Measurements of effective decay rates at various hydrogen partial pressures allow us to determine natural lifetimes and quenching coefficients with molecular hydrogen of several states of small admixtures of rare gases (He, Ne, Ar, Kr). Fig. 2 is a Stern-Volmer plot for the Kr $2p_2$ state. The quenching coefficient is given by the slope and the natural lifetime by the axis intercept at zero molecular hydrogen pressure. The agreement with results from TALIF measurements by Niemi et al. [12] is very good. PROES measurements based on electron impact excitation are, in contrast to laser measurements, not limited by optical selection rules or large energy gaps between the ground and excited state. Therefore, measurements of quenching coefficients of helium and neon states with molecular hydrogen are possible for the first time. Results are discussed in ref. [7].

4.2 EEDF and electron densities

The electron energy distribution function (EEDF) is a key parameter for understanding basic RF discharge mechanisms like electron heating, dissociation, excitation and ionization. Measurements of the high energy part of the EEDF responsible for the latter processes are fairly complicated, however, due to the low densities involved and the transient character during the RF cycle.

PROES yields information on the phase and space resolved EEDF of energetic electrons (>12eV) by a comparison of excitation rates of various states of rare gases (small admixtures) with different excitation thresholds and shapes of the electron impact excitation cross-sections. The gained information does not provide a direct

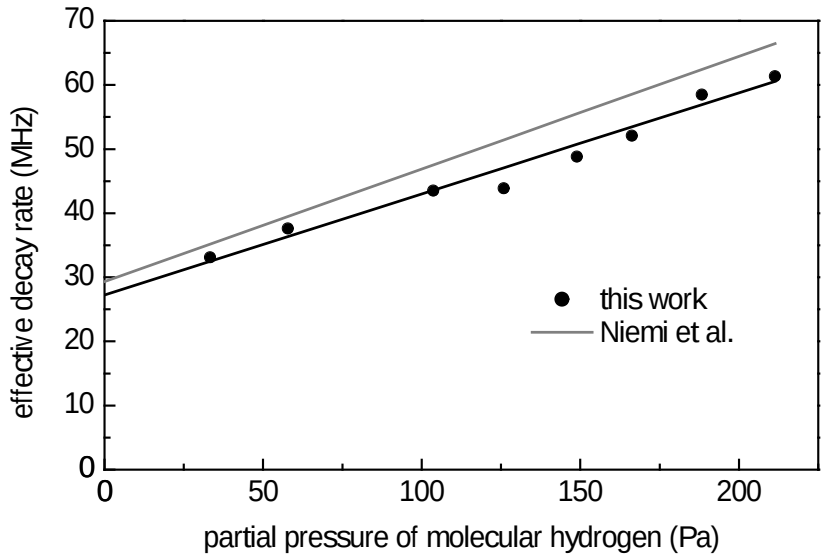

Fig. 2 Effective decay rates for the Kr $2p_2$ state measured by PROES and compared to TALIF (Niemi et al. [12]).

access to the EEDF, however, since the excitation function E_i^e is given by the following integral over the energy dependent electron impact excitation cross section $\sigma_i(E)$ and the EEDF $f(E)$:

$$E_i^e = n_e \int_0^\infty \sigma_i(E) \sqrt{\frac{2E}{m_e}} f(E) dE \qquad . \tag{4}$$

This problem can be overcome by an analytical approach with a set of free parameters describing the shape of the EEDF. This set is varied until the EEDF reproduces the measured excitation functions of all investigated states best. An adapted approach to the investigated discharge is required in general. An appropriate description of electrons in the discharge considered has to allow for a drift component in direction of the electric field in the sheath region. The analysis is based on a shifted Maxwellian distribution function $f_D(E)$ with a drift energy E_D and a single temperature T_e:

$$f_D(E) = \frac{1}{2\sqrt{\pi k_B T_e E_D}} e^{-\frac{(\sqrt{E}-\sqrt{E_D})^2}{k_B T_e}} \left(1 - e^{-\frac{4\sqrt{E}\sqrt{E_D}}{k_B T_e}}\right) \qquad . \tag{5}$$

The parameter sets describing the phase and space resolved EEDFs of directed energetic electrons during the field reversal phase (structure I), the sheath expansion phase (structure II), and of secondary electrons (structure III) are shown in fig. 3. Absolute numbers for the electron density n_e can be determined with the calibrated optical system.

These investigations are possible for the first time, since common diagnostics like Thomson scattering or Langmuir probe measurements are limited by the low densities $\left(10^7 - 10^9 cm^{-3}\right)$ and the transient character of these electrons.

Probe measurements of time independent isotropic low energetic electrons in the plasma bulk show a much higher density $\left(10^{10} cm^{-3}\right)$ of bulk electrons. Their influence on excitation and ionisation processes is negligible, however, due to the low energy $(k_B T_e = 1eV)$ in contrast to the transient electrons measured by PROES.

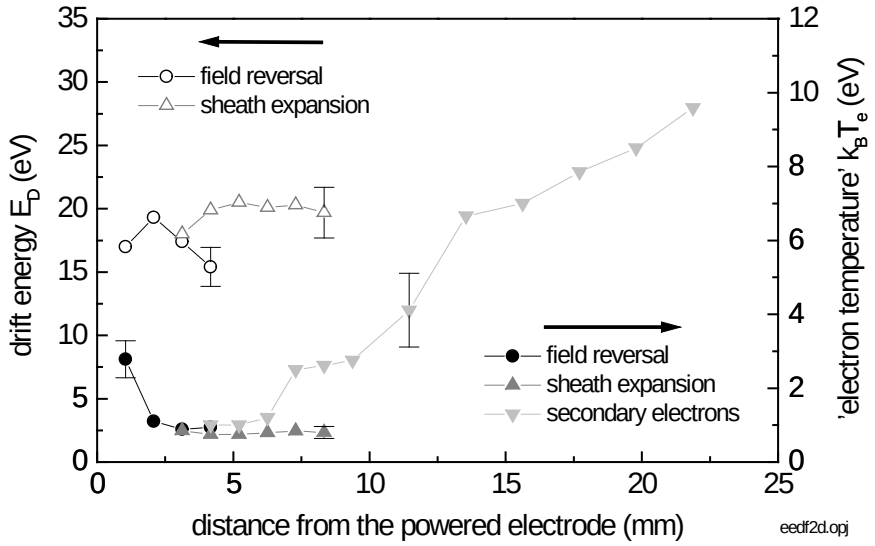

Fig. 3 Parameter sets describing the phase and space resolved EEDF for the various excitation processes.

4.3 Degree of dissociation / atomic densities

For actinometric measurements of atomic densities at a low degree of dissociation, dissociative excitation has to be taken into account [13, 14]. That requires information on the shape of the EEDF. Excitation processes in the discharge under consideration are dominated by directed energetic electrons, as investigated in 4.2. Using the EEDF of time independent low energetic bulk electrons, which can be measured by Langmuir probes, would therefore, crucially underestimate the contribution of dissociative excitation. The excitation by energetic electrons and the low degree of dissociation in the discharge under consideration result in dissociative excitation comparable or even stronger than direct excitation of atoms.

Fig. 4 gives the measured degree of dissociation as a function of the distance from the powered electrode. Excitation by electrons during the field reversal phase and during the sheath expansion phase consists of about 30 percent direct excitation of atoms allowing us to determine the degree of dissociation in the sheath region. Excitation in the plasma bulk, however, is dominated by high energetic secondary electrons resulting in about 90 percent dissociative excitation. Actinometry is not applicable in this region, because the direct contribution is too low for sensitive measurements. The obtained results for the degree of dissociation in the sheath region compare well to direct measurements by TALIF in the same discharge [15].

4.4 Influence of cascading processes on rotational distributions and measurements of the gas temperature

The gas temperature in molecular discharges can be obtained by OES measurements of rotational distributions [11]. The distribution in the ground state is assumed to be characterized by a rotational temperature equal to the gas temperature for low rotational quantum numbers. This distribution is transfered by electron impact excitation into excited states which are observable by OES. Additional population of these states by cascade processes from higher electronic states is commonly neglected.

PROES allows us to check this assumption by investigations of the dynamics of rotational distributions during the RF cycle. Fig. 5 shows the gas temperature calculated with the common model assumptions for various phases of the RF cycle. A strong time dependence caused by cascade processes is observable. The solid line

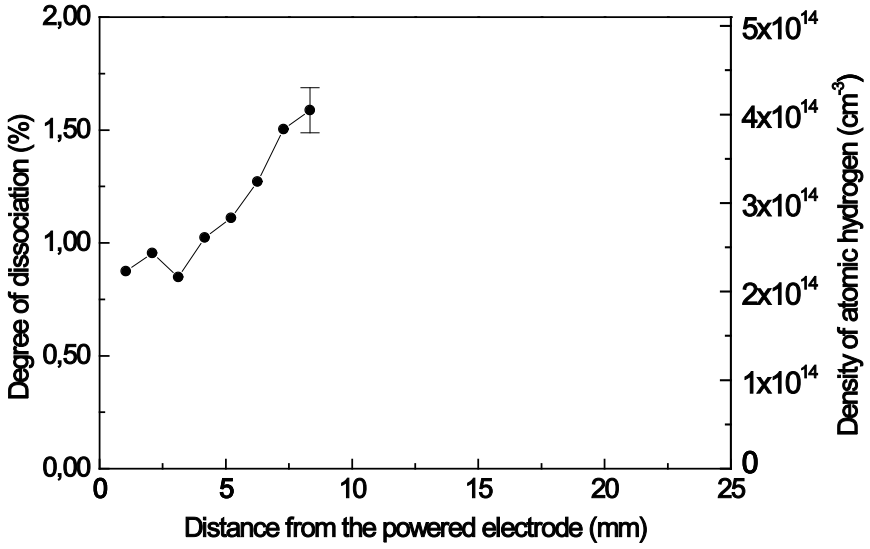

Fig. 4 Axial dependence of the degree of dissociation.

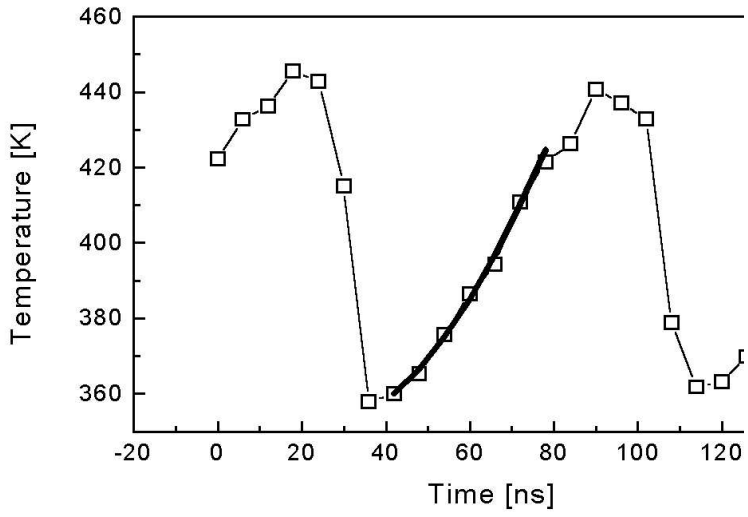

Fig. 5 Formally derived "gas temperatures" infered from Fulcher-α intensities (v=2, N=1-5) of rotational lines demonstrating the importance of cascade processes.

represents a model calculation for the dynamics of rotational distributions with a cascade contribution of eight percent [11]. The strong time dependence is well described by the model.

The best approximation to the gas temperature is the lowest value which is observed at the phase of maximum electron impact excitation ($t \approx 40ns$), when the neglected cascade contribution is smallest. Phase averaged OES measurements result in only slightly overestimated gas temperatures, because phases of strong electron impact excitation and small cascade contribution have higher weights [11].

Acknowledgement

The authors thank Chun C. Lin (University of Wisconsin, Madison) for helpful discussions and C. Fischer and J. Leistikow for skillful technical assistance. Support by the DFG in the frame of SFB 191 is gratefully acknowledged.

References

[1] M.A. Lieberman and A.J. Lichtenberg, *Principles of Plasma Discharges and Materials Processing*, John Wiley & Sons Inc., New York (1994)
[2] H.M. Katsch, E. Quandt and Th. Schneider, Plasma Phys. Control. Fusion **38**, 183 (1996)
[3] I.P. Bogdanova and S.V. Yurgenson, Opt. Spektrosk. **61**, 241 (1986)
[4] J.E. Chilton, J.B. Boffard, R.S. Schappe, and C.C. Lin, Phys. Rev. A **57,** 267 (1998)
[5] J.E. Chilton, M.D. Stewart, Jr., and C.C. Lin, Phys. Rev. A **62** (2000) 32714
[6] J.E. Chilton, M.D. Stewart, Jr., and C.C. Lin, Phys. Rev. A **61** (2000) 52708
[7] T. Gans, Chun C. Lin, V. Schulz-von der Gathen, and H.F. Döbele, Phys. Rev. A **67**, 012707 (2003)
[8] U. Czarnetzki, D. Luggenhölscher, and H.F. Döbele, Plasma Sources Sci. Technol. 8 (1999) 230
[9] T. Gans, Chun C. Lin, V. Schulz-von der Gathen, and H.F. Döbele, J. Phys. D: Appl. Phys., 34 (2001) L39
[10] T. Gans, V. Schulz-von der Gathen, U. Czarnetzki, and H.F. Döbele, Contr. Plasma Phys. 42 (2002) 596
[11] T. Gans, V. Schulz-von der Gathen, and H.F. Döbele, Plasma Sources Sci. Technol., 10 (2001) 17
[12] K. Niemi, V. Schulz-von der Gathen, and H.F. Döbele, J. Phys. D: Appl. Phys. 34 (2001) 2330
[13] H.M. Katsch, A. Tewes, E. Quandt, A. Goehlich, T. Kawetzki, and H.F. Döbele, J. Appl. Phys. 88 (2000) 6232
[14] V. Schulz-von der Gathen and H.F. Döbele, Plasma Chem. Plasma Process. 16 (1996) 46
[15] V. Schulz-von der Gathen, M. Abdel-Rahman, T. Gans, and H.F. Döbele, ICPIG XXVI (2003), Greifswald, Germany